Article

Role of Transporters and Enzymes in Metabolism and Distribution of 4-Chlorokynurenine (AV-101)

Waseema Patel, Ravi G. Shankar, Mark A. Smith, H. Ralph Snodgrass, Munir Pirmohamed, Andrea L. Jorgensen, Ana Alfirevic, and David Dickens*

Cite This: https://doi.org/10.1021/acs.molpharmaceut.3c00700

Read Online

ACCESS | Metrics & More | Article Recommendations | SI Supporting Information

ABSTRACT: 4-Chlorokynurenine (4-Cl-KYN, AV-101) is a prodrug of a NMDA receptor antagonist and is in clinical development for potential CNS indications. We sought to further understand the distribution and metabolism of 4-Cl-KYN, as this information might provide a strategy to enhance the clinical development of this drug. We used excretion studies in rats, *in vitro* transporter assays, and pharmacogenetic analysis of clinical trial data to determine how 4-Cl-KYN and metabolites are distributed. Our data indicated that a novel acetylated metabolite (*N*-acetyl-4-Cl-KYN) did not affect the uptake of 4-Cl-KYN across the blood–brain barrier via LAT1. 4-Cl-KYN and its metabolites were found to be renally excreted in rodents. In addition, we found that *N*-acetyl-4-Cl-KYN inhibited renal and hepatic transporters involved in excretion. Thus, this metabolite has the potential to limit the excretion of a range of compounds. Our pharmacogenetic analysis found that a SNP in *N*-acetyltransferase 8 (*NAT8*, rs13538) was linked to levels of *N*-acetyl-4-Cl-KYN relative to 4-Cl-KYN found in the plasma and that a SNP in *SLC7A5* (rs28582913) was associated with the plasma levels of the active metabolite, 7-Cl-KYNA. Thus, we have a pharmacogenetics-based association for plasma drug level that could aid in the drug development of 4-Cl-KYN and have investigated the interaction of a novel metabolite with drug transporters.

KEYWORDS: *4-chlorokynurenine, N-acetyl-4-chlorokynurenine, N-acetyltransferase, NAT8, SLC7A5, NMDAR*
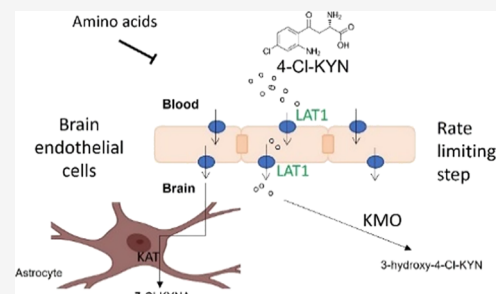
INTRODUCTION

Major depressive disorder is an illness affecting millions of people worldwide, with approximately 3.8% of the population affected. The disorder is characterized by a myriad of symptoms including feelings of low mood, fatigue, insomnia, and anhedonia.[1] Despite the high incidence of the disorder, current treatment regimens are unable to treat up to one-third of patients. Furthermore, in patients who benefit, a process of trial and error may be required to determine the best dose and drug for them resulting in a lag time of weeks or even months between the initiation of treatment and improvement in symptoms.[2]

Recent advances in intervention strategies for depression have focused on the glutamatergic system as a target for medicine development. Examples include 4-chlorokynurenine (4-Cl-KYN), esketamine, and SLS-002.[1,3−6] Indeed, 4-Cl-KYN, a chlorinated form of kynurenine, a tryptophan derivative, has been investigated as an antidepressant with potential for treatment for post-traumatic stress disorder.[7,8] 4-Cl-KYN is thought to bring about antidepressant effects via antagonism of the glycine_B site of the NMDA receptor (NMDAR). Specifically, 4-Cl-KYN is metabolized to the active metabolite, 7-chlorokynurenic acid (7-Cl-KYNA), within astrocytes in the CNS and this active compound then causes antagonism of the NMDAR. Preclinical data from rat studies

have shown that 4-Cl-KYN can have rapid antidepressant effects.[4]

However, in spite of the promising preclinical data on 4-Cl-KYN as an antidepressant, 4-Cl-KYN was unsuccessful in two phase 2 clinical trials, leading to a re-evaluation of its antidepressant properties in humans.[8,9] The compound is still in clinical development in combination with probenecid (NCT05280054) to determine if this boosts the CNS concentration of the active metabolite in humans. This approach is based on a preclinical study in rodents that showed up to 885-fold higher brain extracellular fluid concentration of the active metabolite (7-Cl-KYNA) when probenecid was coadministered with 4-Cl-KYN.[10] Our last study comprehensively characterized the interaction of 7-Cl-KYNA with numerous clinically relevant transporters.[10] This included the probenecid sensitive transporters, OAT3 and MRP4, that are expressed at the rodent BBB and were found to be transporters of 7-Cl-KYNA.[10] Due to several positive

preclinical studies, 4-Cl-KYN has a number of other potential indications including as a therapy for L-DOPA-induced dyskinesias, as an anticonvulsant, and for use in neuropathic pain.[11−14]

In this current study, we wanted to investigate the interaction of a newly discovered metabolite, N-acetyl-4-Cl-KYN (ac-4-Cl-KYN), with clinically relevant drug transporters. Furthermore, we sought to take advantage of the ELEVATE clinical cohort data (NCT03078322) to determine whether pharmacogenetic evaluation of our study cohort could provide novel insights into the relationship between drug concentrations and single-nucleotide polymorphisms (SNPs). This pharmacogenetics approach may enable a personalized medicine strategy for 4-Cl-KYN drug development and dosing.

■ METHODS

Cell Culture. HEK 293 cells were grown at 37 °C in a 5% CO_2-humidified chamber. Cells were cultured in Dulbecco's modified Eagle's media (DMEM) supplemented with 10% fetal bovine serum (FBS).

Stable Cell Line Generation. HEK 293 cell lines stably expressing L-type amino acid transporter (LAT) 1, and organic anion transporters 1, 2, and 3, were generated via stable transfection using Lipofectamine 2000 according to the manufacturer's instructions, as described previously.[10,15] In summary, transporters of interest (OAT1; NM_004790, OAT2 (NM_006672.3), and OAT3; NM_001184732, or vector only) in the pcDNA3.1+/C-(K)DYK vector were introduced into HEK 293 cells, and cells expressing the vector were then selected for using G418 resistance. Selected cells were expanded, and single-cell colonies were isolated. Cells from colonies with the highest expression were validated by using qPCR and further expanded for use in experiments.

Transient Transfections. HEK 293 cells transiently expressing the transporters, human OAT1 (NM_004790) human OAT2 (NM_006672.3), human OAT3 (NM_001184732), OATP1B1 (NM_006446), rat (r) OAT1 (NM_017224.2), rOAT2 (NM_053537.2), and rOAT3 (NM_031332.1), or the matched empty vector (pcDNA3.1+/C-(K)DYK), were generated using Lipofectamine 2000 according to the manufacturer's instructions. Briefly, HEK 293 cells were seeded at a density of 1×10^6 cells/well the day before being transfected. Cells were then transfected with 2.5 μg of DNA/well and experiments conducted 24 h after transfection.

Drugs and Radiochemicals. 7-Cl-KYNA was obtained from Abcam and dissolved in a small volume of 1 M HCl, and the pH was then titrated to 7.4 in PBS. 4-Cl-KYN and ac-4-Cl-KYN were kind gifts from Vistagen Therapeutics, Inc. All other compounds were purchased from Sigma-Aldrich and solubilized in dimethyl sulfoxide according to the manufacturer's instructions.

[^{14}C]-4-Cl-KYN (specific activity = 55.5 mCi/mmol) and [^{14}C]-7-Cl-KYNA (specific activity = 77.7 mCi/mmol) were purchased from Moravek Inc. [^{14}C]-Tetraethylammonium specific activity = 3.5 mCi/mmol) and [^{3}H]-estrone-3-sulfate specific activity = 49.19 Ci/mmol) were purchased from PerkinElmer. [^{3}H]-Phenylalanine (specific activity = 100 Ci/mmol), [^{3}H]-para-aminohippuric acid (specific activity = 40 Ci/mmol), and [^{3}H]-cyclic guanosine monophosphate (specific activity = 25 Ci/mmol) were obtained from American Radiolabeled Chemical Inc. Finally, [^{3}H]-L-DOPA (specific

activity 4 Ci/mmol) was acquired from American Radiolabeled Chemicals, Inc.

Trans-Stimulation Assays. HEK 293 cells stably expressing either LAT1 or a matched empty vector were plated the day before an experiment; cells were 90% confluent at the time of the experiment. Culture media were first aspirated off the cells, and cells were then washed with Hanks' solution. Next, HEK 293 cells were exposed to radiolabeled substrate (L-DOPA) for 3 min at 37 °C, following which excess substrate was removed, and cells were again washed with Hanks' solution. Cells were then exposed to unlabeled substrate for 3 min at 37 °C and excess substrate again removed. Finally, cells were washed with an ice-cold Hanks' solution. To determine intracellular radioactivity, cells were lysed with 5% sodium dodecyl sulfate (SDS) and scintillation fluid was added.[10,16]

Data are presented as mean ± SD unless otherwise stated. Data from trans-stimulation assays were analyzed by one-way ANOVA. A p value <0.05 was considered statistically significant. Analyses were carried out on GraphPad Prism v8.

Radiolabeled Uptake Assays. HEK 293 cells were plated either 1 or 2 days before an experiment, dependent on whether cells stably or transiently expressed the transporter of interest. Cell culture media were removed at the start of each experiment, and cells were washed with Hanks' balanced salt solution (25 mM HEPES, pH 7.4). Cells were then exposed to the radiolabeled compound of interest at a concentration of 0.15 μCi/mL for 3 min at 37 °C. Excess radiolabeled substrate was then removed, and cells were washed with ice-cold Hanks' to prevent further uptake. Intracellular uptake of the radiolabeled compound was determined by lysing cells with 5% SDS and adding scintillation fluid.[10,16]

Data are presented as mean ± SD unless otherwise stated. Data from uptake assays were analyzed by one-way ANOVA. A p-value <0.05 was considered statistically significant. Analyses were carried out on GraphPad Prism v8.

Western Blotting Studies. HEK 293 cells were transiently transfected with human or rat OATs as described in transient transfection. 24 h after transient transfection, cells were washed with ice-cold PBS and incubated with radioimmunoprecipitation assay (RIPA) buffer containing protease inhibitors. The lysates were centrifuged at 18,000g for 30 min at 4 °C to remove cell debris, and the subsequent supernatant was used for Western blot studies. Protein lysates were heated to 37 °C for 20 min, after which protein lysates were loaded onto a 10% polyacrylamide gel, separated by SDS-PAGE, and then transferred to a polyvinylidene fluoride (PVDF) membrane. The membranes were incubated with 5% nonfat dry milk in Tris-buffered saline containing 0.1% Tween 20 (TBST) for 1 h. Membranes were then rinsed with TBST and incubated with an anti-FLAG rabbit polyclonal antibody (1:2000, abcam ab1162) to probe for OATs or a mouse monoclonal antibody (1:4000, Sigma A2228) to probe for β-actin overnight at 4 °C. Membranes were again washed with TBST, after which the membranes were incubated with antirabbit IgG (1:3000, Cell Signaling 7074) or antimouse IgG (1:4000 Cell Signaling 7076) HRP-linked antibody to probe for FLAG tag and β-actin, respectively. Blots were developed using a Pierce-enhanced chemiluminescence substrate and processed using ImageJ software. ImageJ was used to perform the semi-quantitative analysis of the expression of the OAT expression. In brief, densitometric quantification for OATs was carried out by selecting a region of interest (ROI) around the band at the expected size of 75 kDa and smear due to post-translational

modifications.[17−19] The ROI was used to determine the density of the band and smear (mean gray value within the region); the same ROI was used across all bands/smears. Changes in the expression of β-actin were determined in the same way. Changes in the expression of the OATs were then normalized to β-actin and are shown relative to the level of the OAT expression in control cells (FLAG).

Excretion Mass Balance and Metabolite Identification Study. Animal experiments were conducted by Charles Rivers Laboratories (Ashland, USA) with approval from their Institutional Animal Care and Use Committee. Food and water were made available to animals *ad libitum*. To determine the excretion of [^{14}C]-4-Cl-KYN and/or metabolites, three male and three female Sprague−Dawley rats were orally dosed (gavage) with 500 mg/kg and 100 μCi/kg to determine routes of elimination and excretion mass balance. Following dosing, animals were placed into metabolism cages for separate collection of urine and feces through 7 days. Following dosing, all excretion mass balance animals were placed in plastic metabolism cages for separate collection of urine and feces. Samples were analyzed for total radioactivity by liquid scintillation counting (LSC).

For the metabolite identification study, Sprague−Dawley rats were dosed with a single oral dose of [^{14}C]-4-Cl-KYN at 500 mg/kg and a target radioactivity of 250 μCi/kg. At 1 and 4 h post dose, blood samples were collected from one animal/ sex/time point. Selected plasma samples were profiled for metabolites using radiomatic HPLC comprising a β-Ram model 4B radiomatic detector (IN/US Systems, Inc., Florida, USA) and a Zorbax SB-C18 column. Metabolites representing ≥5% of the total radioactivity (plasma) were analyzed by radio-HPLC/mass spectrometry (MS)−MS to identify the radiolabeled metabolites.

Clinical Study Cohort. A subset of study participants from the ELEVATE (ClinicalTrials.gov Identifier: NCT03078322) trial, who provided informed written consent for pharmacogenetic analysis, were used for our study. Participants were recruited from across the United States and were of mixed ethnic background, aged between 18 and 65 years. Trial participants had been previously diagnosed with major depressive disorder and were currently experiencing a depressive episode of at least 8 weeks in duration. For the trial, participants took a placebo or one oral dose of 4-Cl-KYN (1.44 g) in the morning after no/light breakfast in addition to an antidepressant prescribed by their doctor for 2 weeks. A blood sample was taken from participants after taking an oral dose of 4-Cl-KYN.

The time between administration of 4-Cl-KYN and blood sample taking was recorded. For each individual patient, at least one additional blood sample was taken on a separate occasion. 4-Cl-KYN, ac-4-Cl-KYN, and 7-Cl-KYNA plasma concentrations were determined using HPLC with MS/MS detection by MicroConstants (San Diego, USA). In brief, the method is applicable for measuring concentrations of 4-Cl-KYN, ac-4-Cl-KYN, and 7-Cl-KYNA ranging from 50.0 to 50,000, 10.0 to 10,000, and 2.00 to 2,000 ng/mL, respectively, using 40.0 μL of human plasma for extraction. The extracts were analyzed by HPLC using a Phenomenex Synergi MAX-RP column. The mobile phase was nebulized using heated nitrogen in electrospray positive ionization mode, and the compounds were detected using MS/MS.

Genotyping and Imputation. Genotyping was performed by Genuity Science (Dublin, Ireland) using an Illumina

Infinium global screening array. The tool gtc2vcf (Giulio Genovese, 2022, URL-https://github.com/freeseek/gtc2vcf) was used to convert intensity data files into VCF files for downstream analyses. Standard GWAS quality control was performed against the genotype data using PLINK 1.9 (https://zzz.bwh.harvard.edu/plink/cite.shtml) to filter out SNPs and individuals. The steps included removing samples with >1% missingness, duplicates or related samples, outlying homozygosity values, sex discordance, and removal of ancestry outliers. Variant-level checks removed SNPs with lower minor allele frequency and statistically significant Hardy−Weinberg equilibrium values. The Michigan Imputation Server (https://github.com/genepi/imputationserver) was used for genotype imputation, as some of the SNPs to be investigated were not directly genotyped. The 1000 Genomes Phase 3 version 5 reference panel was used for the imputation. A total of 98 patient samples passed quality control analyses and were taken forward for analysis.

Due to the sample size, a targeted analysis based on a candidate gene approach for key SNPs was performed. Selected SNPs, from associations in metabolome-wide association studies (MWAS) that have been linked to the plasma level of the nonchlorinated derivatives of the kynurenine pathway, are summarized in Table 1. These SNPs were evaluated in a targeted analysis for association testing of SNPs and plasma concentrations.

Table 1. Association Testing Plan

individual drug	gene	genotyping	reason for testing
4-Cl-KYN	SLC7A5 (rs28582913)	imputation	Shin et al. (2014) and Long et al. (2017)
7-Cl-KYNA	KMO (rs61825638)	imputation	Shin et al. (2014) and Long et al. (2017)
	SLC7A5 (rs28582913)	imputation	Shin et al. (2014), Long et al. (2017), and Patel et al. (2021)
ac-4-Cl-KYN	NAT8 (rs13538)	direct	Yin et al. (2022)

drug ratios	gene	genotyping	reason for testing
7-Cl-KYNA/4-Cl-KYN	KMO (rs61825638)	imputation	Shin et al. (2014) and Long et al. (2017)
	SLC7A5 (rs28582913)	imputation	Shin et al. (2014), Long et al. (2017), and Patel et al. (2021)
ac-4-Cl-KYN/4-Cl-KYN	NAT8 (rs13538)	direct	Yin et al. (2022)

Analysis for Association between SNPs and Plasma Concentrations. The outcome variables we investigated were the plasma concentrations of 4-Cl-KYN, 7-Cl-KYNA, ac-4-Cl-KYN, and the ratios of 7-Cl-KYNA:4-Cl-KYN and ac-4-Cl-KYN:4-Cl-KYN. We used a regression modeling framework like that employed by researchers investigating clozapine and its metabolites.[20] Briefly, we tested for an association between these outcomes and SNPs of interest (Table 1) using a linear fixed effects model and a random effect at the subject level. Confounding variables such as the time difference between drug being taken and blood being collected, age, ethnicity, and visit, were considered univariately. The model used to test for association between plasma concentrations and SNPs then
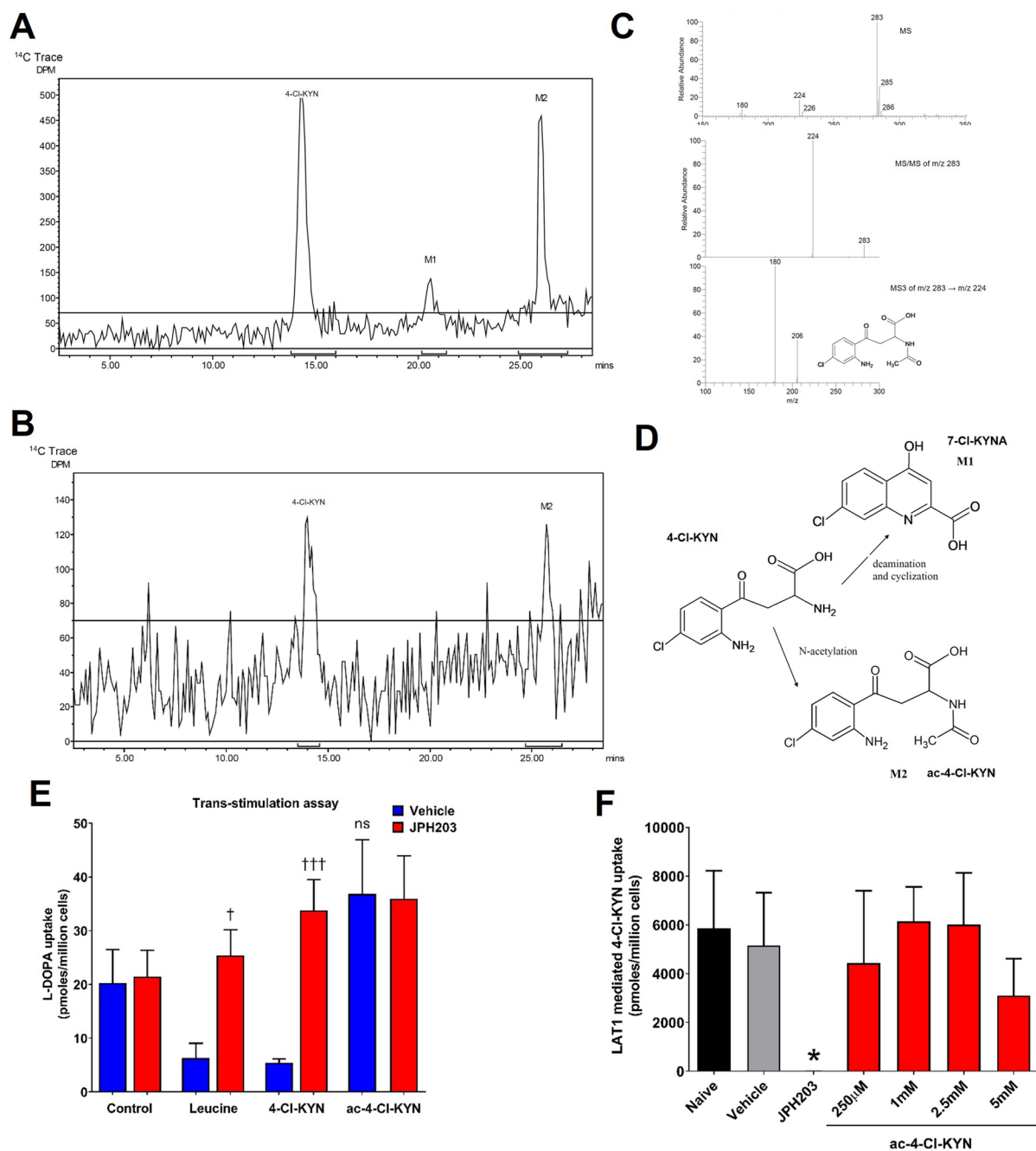
Figure 1. LAT1 transport is not affected by the novel metabolite, *N*-acetyl-4-chlorokynurenine. Representative HPLC radiochromatogram of plasma from Sprague−Dawley rat at the (A) 1 h or (B) 4 h time point following oral administration of $[^{14}C]$-4-Cl-KYN. (C) Mass spectrometry analysis of novel metabolite peak (M2) from rat plasma to ID metabolite as an *N*-acetylated derivative of 4-Cl-KYN. (D) Schematic for the metabolism of 4-Cl-KYN to the active metabolite (7-Cl-KYNA, M1) or acetylation to generate ac-4-Cl-KYN (M2). (E) HEK 293-LAT1 cells were preloaded with [3H]-levodopa (L-DOPA; 1 μM) and then exposed to 1 mM leucine, 4-Cl-KYN, or *N*-acetyl-4-chlorokynurenine (ac-4-Cl-KYN) in the presence or absence of the inhibitor JPH203 (10 μM). (F) Uptake of $[^{14}C]$-4-Cl-KYN in HEK 293 cells under the conditions indicated. LAT1-mediated uptake of 4-Cl-KYN was determined by subtracting the uptake in HEK 293 control cells from the uptake in HEK 293-LAT1. Cells were exposed 250 μM 4-Cl-KYN in the presence of the concentrations of ac-4-Cl-KYN indicated. Data are mean ± SD (n = 3). †$p < 0.05$, †††$p < 0.001$ compared to matched vehicle-treated cells. *$p < 0.05$ compared to naïve cells. ns = no significant difference compared to vehicle control ($p > 0.05$).

included the random effects at subject level and the variables found significant univariately, as well as the first two principal components of population structure. Where the distribution of plasma concentrations was non-Gaussian, the data were transformed by using either the $\log_{10}$ or square-root transformation, as appropriate. Due to the seven tests for association undertaken, we set our significance threshold to 0.05/7 = 0.0071 to reflect a Bonferroni correction for multiple testing.

In Silico Docking. The AlphaFold predictive structure of human NAT8 (Q9UHE5-F1 v4) was used as a template for *in silico* docking. Identification of a putative docking pocket was determined with AMDock (ver 1.5.2) software[21] in an unbiased manner. In brief, 4-Cl-KYN and acetyl-CoA were docked with NAT8 using AutoDock Vina[22] within AMDock
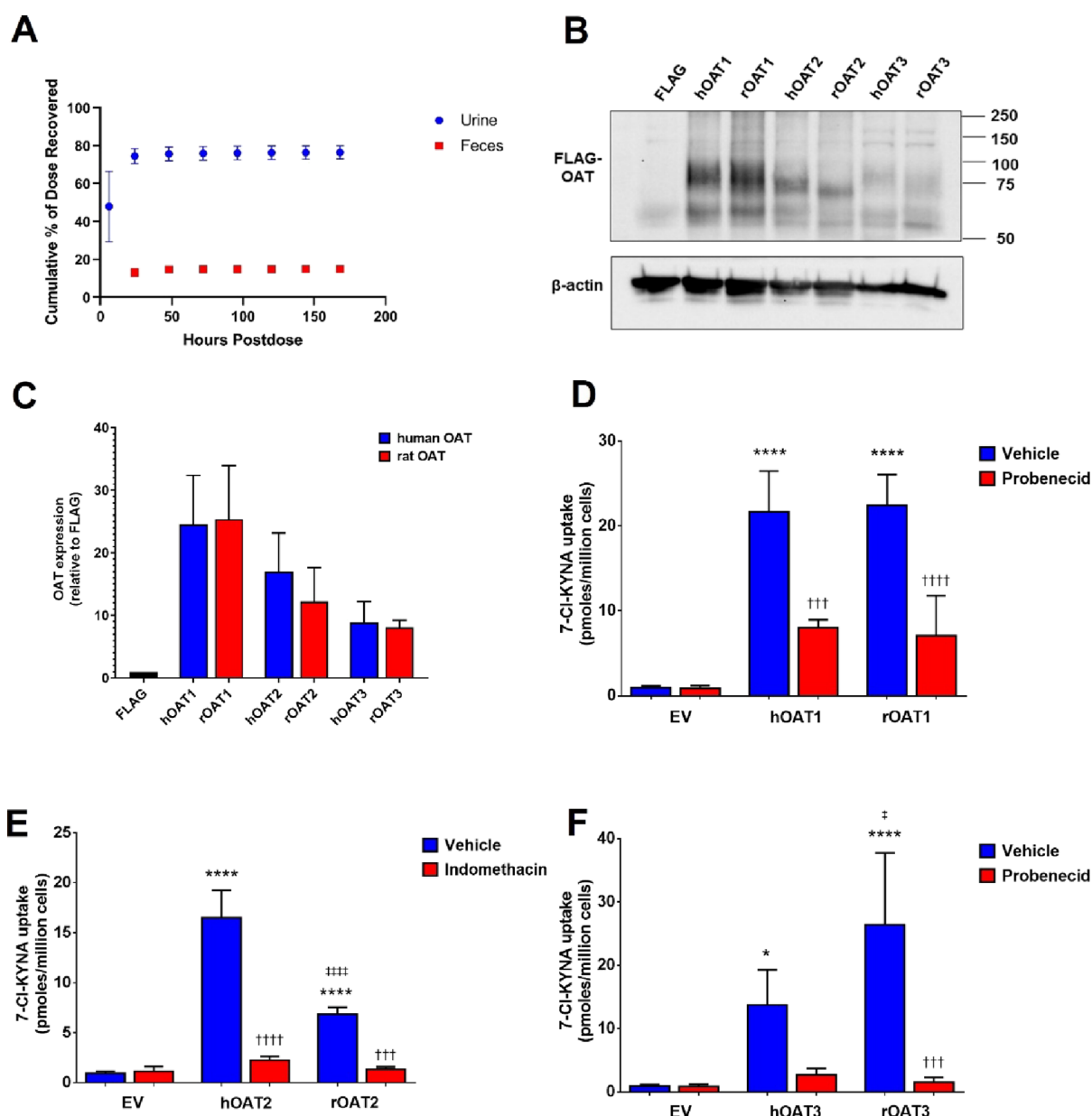
Figure 2. Differences in the uptake of 7-Cl-KYNA between human and rat organic anion transporters. (A) Routes of elimination and excretion mass balance of [^{14}C]-4-Cl-KYN-derived radioactivity in Sprague–Dawley rats following a single oral dose. Data are mean ± SD ($n = 6$). (B) Representative Western blot images showing the expression of human and rat FLAG-OATs under conditions indicated. (C) Densiometric quantification of the expression of OATs under conditions indicated. Densiometric quantification for the OATs was carried out using the band at the expected size of 75 kDa and smear due to post-translational modifications. Changes in the expression of OATs were normalized to β-actin and are shown relative to OAT expression in control cells (FLAG). Data are mean ± SD ($n = 3$). (D–F) Uptake of [^{14}C]-7-chlorokynurenic acid (7-Cl-KYNA) under conditions indicated in control HEK 293 cells and HEK 293 cells transfected with human (h) or rat (r) organic anion transporter (OAT) (D) 1, (E) 2, or (F) 3. Cells were exposed with 2 μM 7-Cl-KYNA, 100 μM indomethacin, or 1 mM probenecid. Data are mean ± SD ($n = 3$). **$p < 0.01$, ****$p < 0.0001$ compared to empty vector (EV), †$p < 0.05$, ††$p < 0.01$, †††$p < 0.001$, ††††$p < 0.0001$ compared to matched HEK 293-OAT cells, ‡$p < 0.05$ when compared to matched hOAT.

software. The docking pose with the highest energy coefficient was used for generation of images produced in PyMOL (ver 2.52).

■ RESULTS

***N*-Acetyl-4-Chlorokynurenine Does Not Inhibit or Interact with the LAT1 Transporter.** Plasma samples from Sprague–Dawley rats dosed with [^{14}C]-4-Cl-KYN were utilized for metabolite analysis to investigate the pharmacology of 4-Cl-KYN. To determine the number and relative

concentrations of radiolabeled compounds, the plasma samples were profiled using HPLC with radiodetection and mass spectrometry. The primary component present in plasma at the 1 h time point was the parent 4-Cl-KYN, representing approximately 53% relative observed intensity (% ROI) (Figure 1A). The second largest component was M2, an unknown metabolite, eluting at 26 min, representing about 41% ROI. The third largest component from plasma was M1; representing about 6% ROI at the 1 h time point is the known
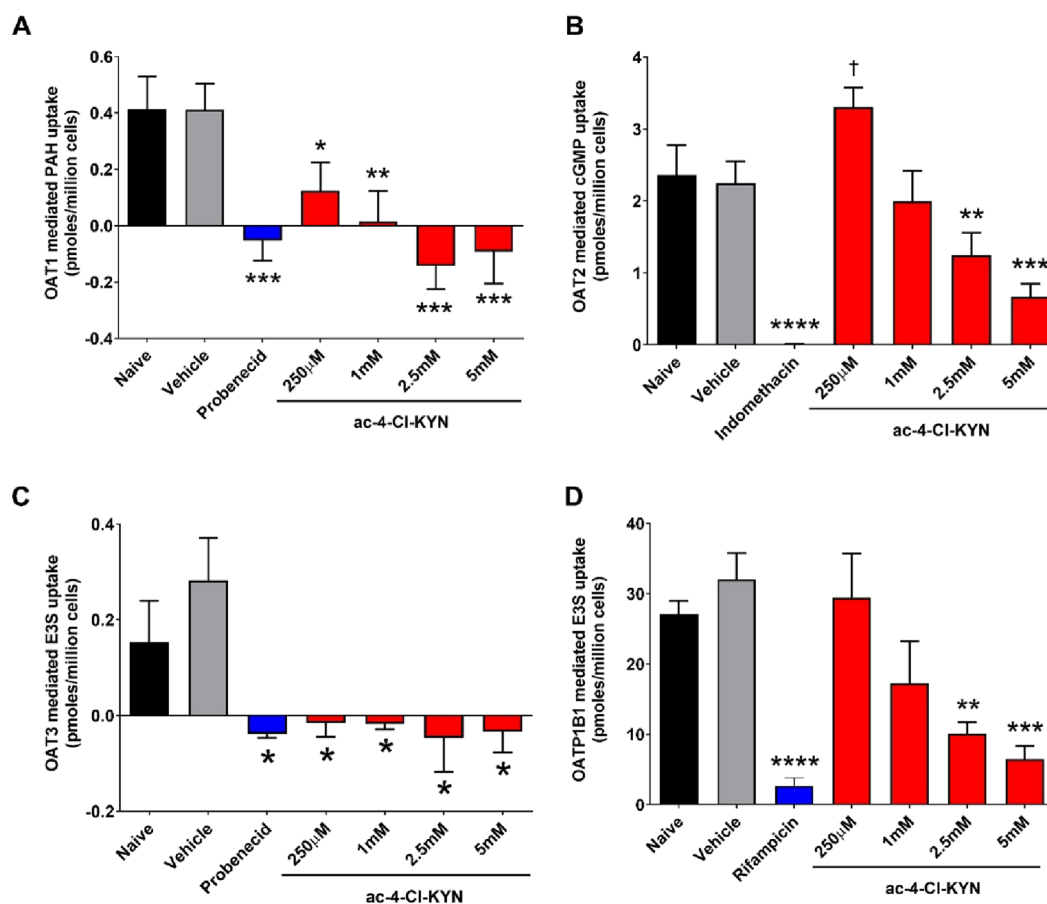
Figure 3. N-Acetyl-4-chlorokynurenine inhibits renal and hepatic transporters. (A) Uptake of $[3H]$-para-aminohippuric acid (PAH; 1 μM) under conditions indicated or 1 mM probenecid. Organic anion transporter (OAT) 1-mediated uptake of PAH was determined by subtracting the uptake in HEK 293 control cells from the uptake in HEK 293-OAT1. (B) Uptake of $[3H]$-cyclic guanosine monophosphate (cGMP) under conditions indicated or 100 μM indomethacin. OAT2-mediated uptake of cGMP was determined by subtracting the uptake in HEK 293 control cells from the uptake in HEK 293-OAT2. (C) Uptake of $[3H]$-estrone-3 sulfate (E3S; 100 nM) under conditions indicated or 1 mM probenecid. OAT3-mediated uptake of E3S was determined by subtracting the uptake in HEK 293 control cells from the uptake in HEK 293-OAT3. Data are mean $\pm$ SD ($n = 3$). (D) Uptake of $[3H]$-estrone-3 sulfate (E3S; 100 nM) under conditions indicated or 100 μM rifampicin. OATP1B1-mediated uptake of E3S was determined by subtracting the uptake in HEK 293 control cells from the uptake in HEK 293-OATP1B1. Cells were exposed to a model substrate in the presence or absence of different chemicals including a range of concentrations for ac-4-Cl-KYN as indicated. Data are mean $\pm$ SD ($n = 3$). *$p < 0.05$, **$p < 0.01$, ***$p < 0.001$, ****$p < 0.0001$ when compared to naïve.

active metabolite, 7-Cl-KYNA. 7-Cl-KYNA was not detected in the 4 h sample (Figure 1B).

Mass spectrometry was utilized to identify the M2 peak. The $(-)$ESI MS spectrum has a $(M-H)-$ ion at $m/z = 283$ with a 37Cl isotope peak at $m/z = 285$ (Figure 1C). The molecular ion is consistent with 4-Cl-KYN that has been acetylated. The MS/MS spectrum of m/z 283 has a single fragment ion at m/z 224 from the loss of NH2COCH3 (Figure 1C). The MS3 spectrum of m/z 283 $\rightarrow$ m/z 224 has fragment ions at m/z 206 from the loss of H_2O and at m/z 180 from the loss of CO_2 (Figure 1B). The mass spectrometry data are consistent with a structure of 4-Cl-KYN that has undergone acetylation at the alpha amino position.

To summarize, the metabolic pathway for 4-Cl-KYN involves either N-acetylation at the alpha amino position to form M2 (N-acetyl-4-Cl-KYN) or 4-Cl-KYN undergoes cyclization with the loss of NH3 to form M1 (7-Cl-KYNA) (Figure 1D).

We then tested the effect of N-acetyl-4-Cl-KYN (ac-4-Cl-KYN) on transporters expressed in the brain and elsewhere. Our previous study investigated the interaction of the active metabolite, 7-Cl-KYNA, with several transporters.[10] We started

by investigating whether ac-4-Cl-KYN could interact with LAT1 (SLC7A5) using a trans-stimulation assay, as this transporter is instrumental in the uptake of 4-Cl-KYN across the BBB. Thus, we preloaded HEK 293 LAT1 cells with a known radiolabeled substrate of LAT1 (L-DOPA), washed out excess substrate, and then exposed cells to potential substrates for LAT1. We found that known substrates of LAT1 (such as leucine and 4-Cl-KYN) caused a reduction in intracellular L-DOPA accumulation due to the antiporter mechanism of LAT1 extruding L-DOPA for uptake of leucine or 4-Cl-KYN. The LAT1 inhibitor, JPH203, prevented the leucine and 4-Cl-KYN induced reduction in intracellular L-DOPA. ac-4-Cl-KYN, however, had no effect on intracellular L-DOPA accumulation, suggesting that it is not a substrate for LAT1 (Figure 1E).

We next tested whether ac-4-Cl-KYN could affect 4-Cl-KYN uptake via LAT1 by acting as an inhibitor by measuring the uptake of 4-Cl-KYN in HEK 293-LAT1 and matched control cells in the presence of a series of concentrations of ac-4-Cl-KYN. 250 μM 4-Cl-KYN was used in this experiment as it is a similar concentration to that found in the plasma of patients taking 4-Cl-KYN in recently completed clinical trials. We found that the LAT1 inhibitor JPH203 caused a reduction in
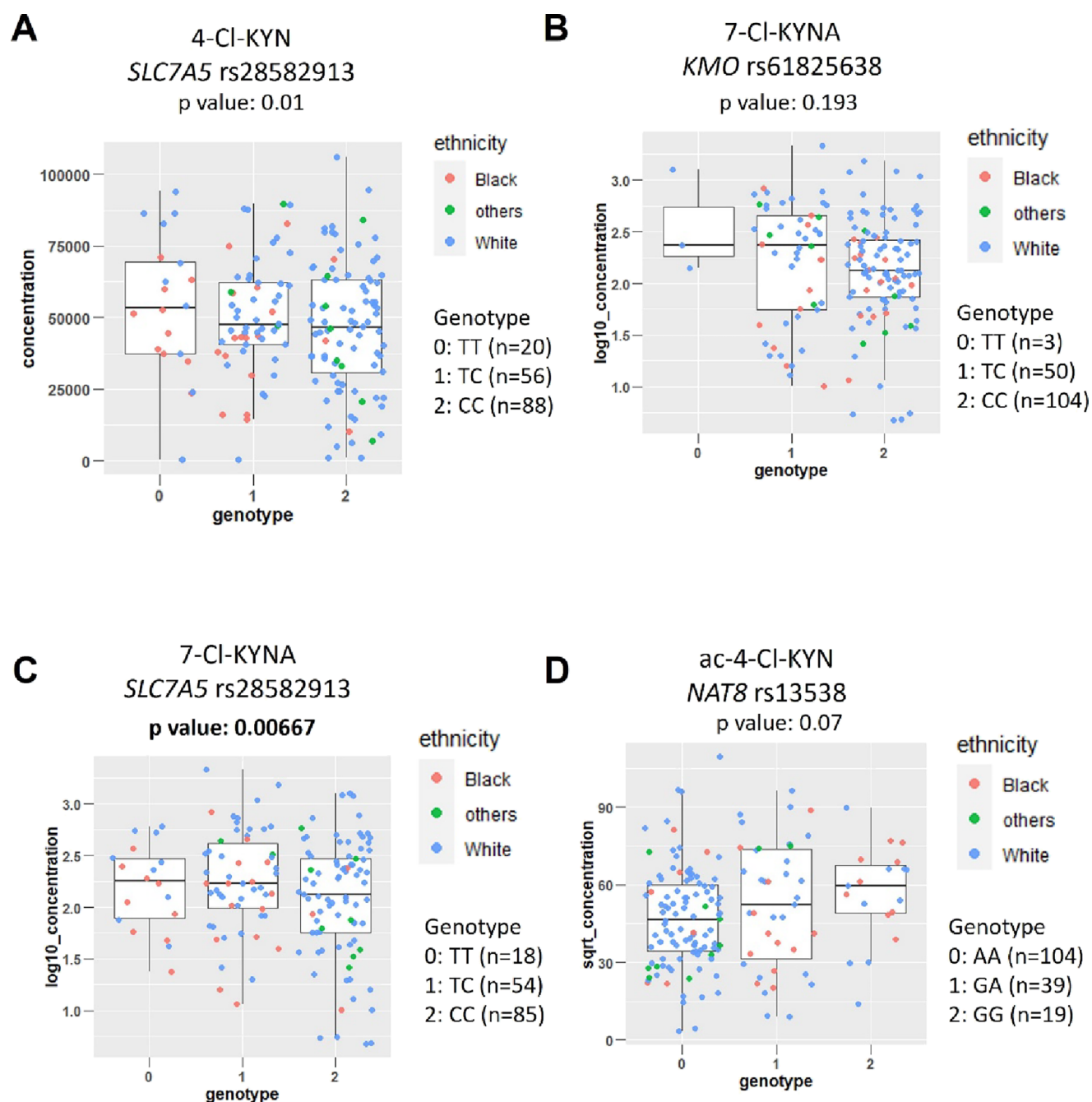
F

Figure 4. 7-Cl-KYNA levels are linked to an *SLC7A5* SNP (rs28582913). (A) Effect of *SLC7A5* SNP (rs28582913) on the plasma level of 4-Cl-KYN (mg/mL). (B) Effect of the *KMO* SNP (rs61825638) on 7-Cl-KYNA plasma levels (Log_{10} ng/mL). (C) Association of 7-Cl-KYNA plasma concentrations with *SLC7A5* SNP (rs28582913) (Log_{10} ng/mL). (D) Effect of *NAT8* SNP (rs13538) on ac-4-Cl-KYN plasma levels (SQRT ng/mL). Plasma levels of compounds of interest were determined from patients participating in the ELEVATE clinical trial. The significance threshold was a Bonferroni-corrected p value for multiple testing of $p < 0.0071$ with significant p values in bold. Self-reported ethnicity is shown with other ethnic background shortened to Others.

the LAT1-mediated uptake of 4-Cl-KYN, but none of the concentrations of ac-4-Cl-KYN tested had any effect (Figure 1F). This data indicated that the presence of ac-4-Cl-KYN does not interfere with LAT1-mediated uptake of 4-Cl-KYN.

4-Chlorokynurenine and Metabolites Are Excreted via Urine. As acetylated metabolites can be subject to renal excretion and as the active metabolite of 4-Cl-KYN (7-Cl-KYNA) is a substrate of renal transporters,[10] we wanted to further understand the distribution of 4-Cl-KYN and/or its metabolites. To investigate this, an *in vivo* excretion mass

balance study was performed in Sprague−Dawley rats following a single oral dose of [^{14}C]-4-Cl-KYN. We found that 4-Cl-KYN and metabolites are primarily excreted via urine, evidenced by 76% [^{14}C]-4-Cl-KYN related radioactivity recovered in urine (Figure 2A). Radioactivity recovered in feces was 14.9%. In both cases, no differences were observed in the excretion of the compound between males and females.

Differences in the Uptake of 7-Cl-KYNA between Human and Rat Organic Anion Transporters. Species differences have been reported for OAT transporters, for

Table 2. Summary of SNP and Blood Concentration Association Testing[a]

individual drug	gene	association p value	SNP coefficient estimate	N
4-Cl-kynurenine (4-Cl-KYN) (ng/mL)	SLC7A5 (rs28582913)	0.01	−7355	164
7-Cl-kynurenic acid (7-Cl-KYNA) (Log$_{10}$ng/mL)	KMO (rs61825638)	0.193	−0.13	157
	SLC7A5 (rs28582913)	**0.00667**	−0.27	157
N-acetyl-4-Cl-kynurinine (ac-4-Cl-KYN) (SQRT ng/mL)	NAT8 (rs13538)	0.07	4.49	162

drug ratios	gene	association p value	SNP coefficient estimate	N
7-Cl-KYNA:4-Cl-KYN (Log$_{10}$ng/mL)	KMO (rs61825638)	0.136	−0.22	157
	SLC7A5 (rs28582913)	0.039	−0.14	157
ac-4-Cl-KYN: 4-Cl-KYN (Log$_{10}$ng/mL)	NAT8 (rs13538)	**0.00608**	0.097	159

[a]Results of testing for association between SNPs and blood concentration of parent or metabolites of 4-Cl-KYN using a linear mixed model regression modeling approach. The significance threshold was a Bonferroni-corrected p value for multiple testing of $p < 0.0071$ with significant p values in bold. The following covariates were adjusted for time from dosing, sex, and ethnicity.
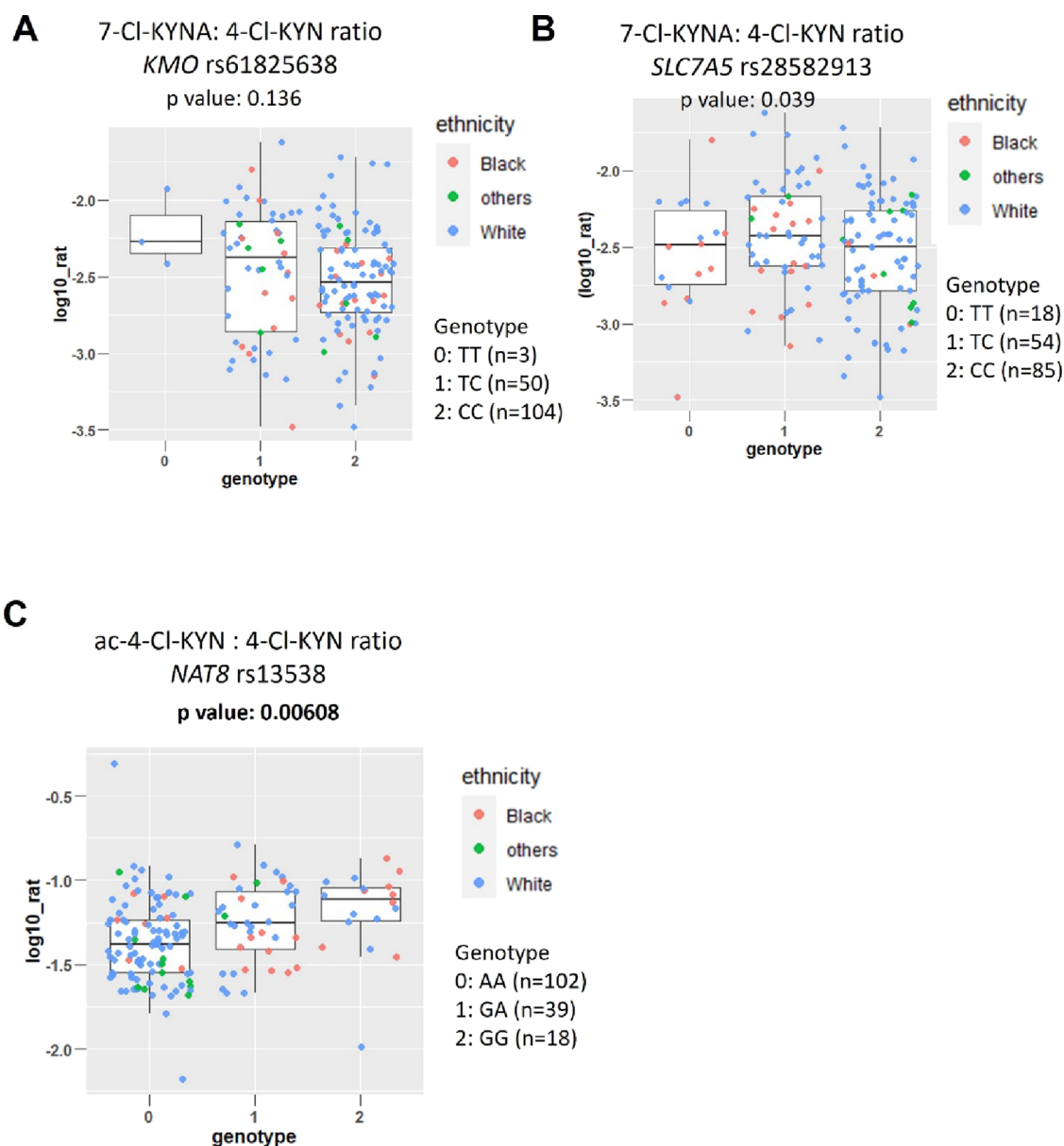

Figure 5. The ac-4-Cl-KYN:4-Cl-KYN plasma ratio is associated with a NAT8 SNP (rs13538). (A) Effect of a KMO SNP (rs61825638) on the plasma ratio of 7-Cl-KYNA:4-Cl-KYN (Log$_{10}$ ng/mL). (B) Effect of a SLC7A5 SNP (rs28582913) on the plasma ratio of 7-Cl-KYNA:4-Cl-KYN (Log$_{10}$ ng/mL). (C) Association of ac-4-Cl-KYN:7-Cl-KYNA plasma ratio with a NAT8 SNP (rs13538) (Log$_{10}$ ng/mL). Plasma levels of compounds of interest were determined from patients participating in the ELEVATE clinical trial. The significance threshold was a Bonferroni-corrected p value for multiple testing of $p < 0.0071$ with significant p values in bold. Self-reported ethnicity is shown with other ethnic background shortened to others.
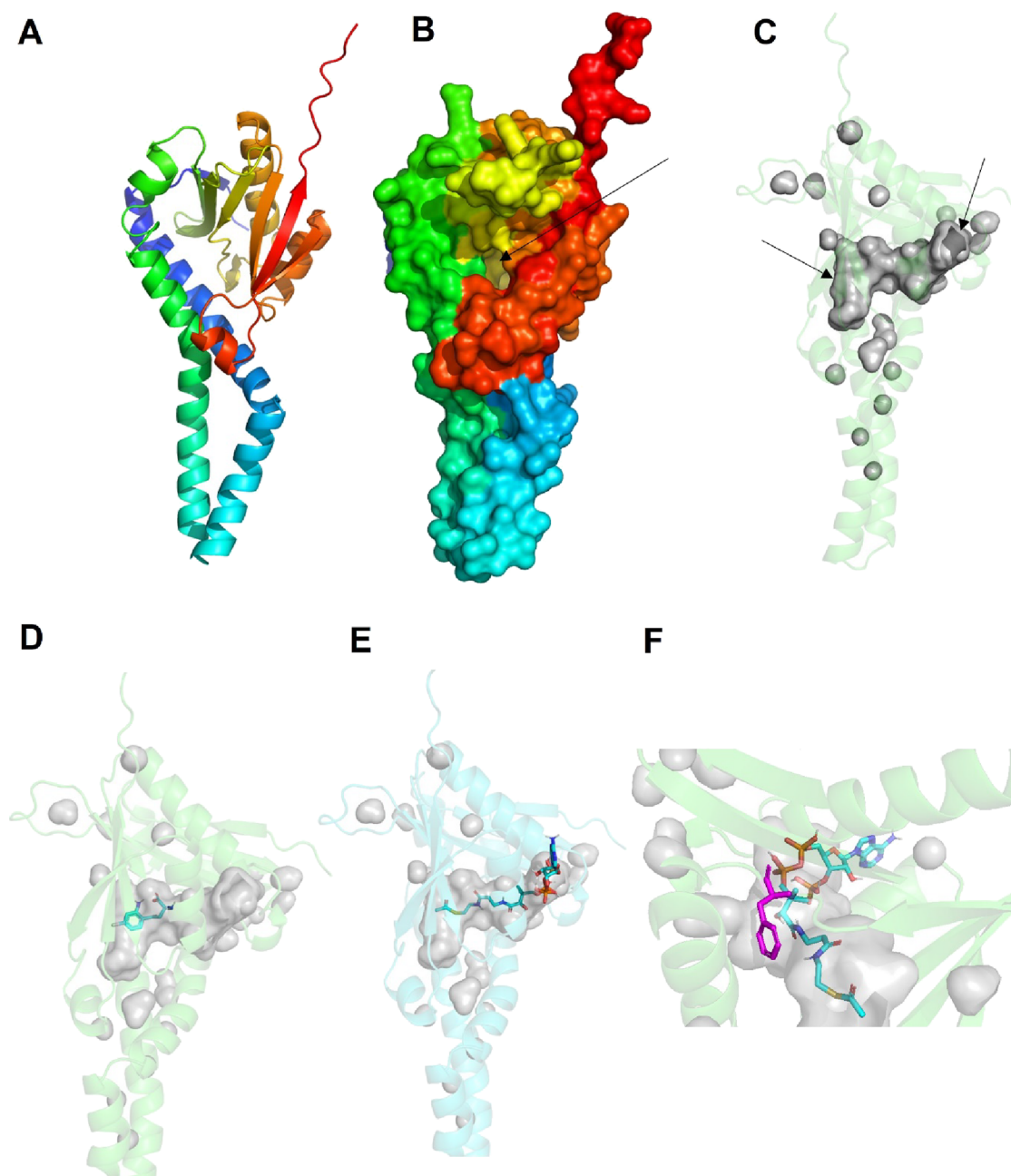
Figure 6. *In silico* docking of 4-Cl-KYN and acetyl-CoA onto NAT8. (A) Overall AlphaFold predicted structure of NAT8 with secondary structures as cartoons. (B) Surface of NAT8 with focus on pore entrance marked by arrow. (C) Solvent-accessible continuous pore of NAT8 in gray with arrows at either end of the channel (active site). Docking of 4-Cl-KYN (D) or acetyl CoA (E) onto NAT8. (F) Location of nonsynonymous SNP (Phe143Ser, rs13538) in purple on NAT8 with docked acetyl CoA.

example human versus rat OATs for the transport of kynurenic acid.[23] We next tested whether there were any species differences in OAT activity toward 7-Cl-KYNA transport. We used transient transfection to introduce human and rat homologues of OAT transporters 1, 2, and 3 (*SLC22A6, SLC22A7, SLC22A8*) into HEK 293 cells. Western blot studies validated the expression of different OAT transporters. A smear for the OAT transporters was observed, which is consistent with posttranslational modifications such as glycosylation and/or ubiquitination that have been previously reported for this transporter family[17−19]. A semiquantitative approach showed that there were no significant differences in

the levels of expression of the different OAT transporters between the human and rat homologues (Figure 2B,C).

We next sought to compare the uptake of 7-Cl-KYNA via the human and rat OATs. 2 μM 7-Cl-KYNA was used in this experiment as it is a similar concentration to that found in the plasma of patients taking 4-Cl-KYN in recently completed clinical trials. On average, we found uptake of 7-Cl-KYNA via hOAT1 (21.7 ± 4.8 pmol/million cells) and rOAT1 (22.5 ± 3.6 pmol/million cells) to be similar and probenecid to have a similar effect on both transporters, 8.0 ± 1.0 and 7.1 ± 4.8 pmol/million cells for hOAT1 and rOAT1, respectively (Figure 2D). Conversely, we found that hOAT2 (16.5 ± 2.8 pmol/million cells) had a higher uptake of 7-Cl-KYNA than

rOAT2 (6.9 ± 0.7 pmol/million cells, Figure 2E, n = 3, p < 0.05). We also found differences in uptake between hOAT3 and rOAT3; hOAT3 (13.8 ± 5.6 pmol/million cells) was found to have a lower uptake of 7-Cl-KYNA than rOAT3 (26.4 ± 11.3 pmol/million cells, Figure 2F, n = 3, p < 0.05). Due to these species differences, we focus additional experiments on human data from *in vitro* or clinical data to further investigate the pharmacology of these compounds.

N-Acetyl-4-chlorokynurenine Inhibits Renal and Hepatic Transporters. We next determined whether the inactive metabolite of 4-Cl-KYN, ac-4-Cl-KYN, could affect other clinically relevant human drug transporters, as this could be important in drug−drug interactions. We started by looking at the renally expressed transporter using our previously established stably expressing cell lines.[10] We found that the presence of ac-4-Cl-KYN caused an inhibition of OAT1 (*SLC22A6*) and OAT3 (*SLC22A8*) mediated uptake of the model substrates para-aminohippuric acid and estrone-3 sulfate, respectively (Figure 3A,C).

We also studied the hepatic transporters, OAT2 (*SLC22A7*) and OATP1B1 (*SLCO1B1*). We found that uptake of the OAT2 model substrate cyclic guanosine monophosphate was reduced in the presence of ac-4-Cl-KYN (Figure 3B). Similarly, OATP1B1-mediated uptake was also reduced in the presence of ac-4-Cl-KYN (Figure 3D). These data, together, indicate that the acetylated metabolite of 4-Cl-KYN is capable of inhibiting human transporters involved in excretion in both the kidneys and liver.

Analyses of Association between SNPs and Individual Drugs. Candidate SNPs, based on prior associations with kynurenine pathway metabolites (Table 1), were investigated for association with the plasma concentrations of 4-Cl-KYN and/or drug metabolites using a regression modeling framework. In univariate analyses with potential confounders, time from dosing was significantly associated with ac-4-Cl-KYN levels (p: 0.000007). The significant factor was adjusted for in the SNP association analyses, together with the first two principal components of ancestry.

No association was found between *SLC7A5* rs28582913 and 4-Cl-KYN (p: 0.01) (Figure 4A) or between *KMO* rs61825638 and 7-Cl-KYNA levels (p: 0.193) (Figure 4B). An association was identified between *SLC7A5* rs28582913 and 7-Cl-KYNA levels (p: 0.00667), and the SNP appeared to have a recessive effect, with two copies of the "C" allele at rs28582913 leading to approximately 46% lower blood concentrations of 7-Cl-KYNA (Figure 4C). Finally, no association was identified between the SNP in *N*-acetyltransferase 8 (*NAT8*; rs13538) and the concentration of ac-4-Cl-KYN (p: 0.07) (Figure 4D and Table 2).

Association between Metabolite: 4-Cl-KYN Ratios and SNPs. In univariate analyses with potential confounders, time from dosing was significantly associated with 7-Cl-KYNA:4-Cl-KYN (p: 0.025) and ac-4-Cl-KYN:4-Cl-KYN (p: 0.00000003) ratios. The significant factor was adjusted for in the SNP association analyses, together with the first two principal components of ancestry.

No association was found between KMO rs61825638 and 7-Cl-KYNA:4-Cl-KYN (p: 0.136), or between *SLC7A5* rs28582913 and 7-Cl-KYNA:4-Cl-KYN (p: 0.039) (Figure 5A,B). A significant association was identified between *NAT8* rs13538 SNP and ac-4-Cl-KYN:4-Cl-KYN (p: 0.00608) (Figure 5C and Table 2). The results suggested that the SNP had an additive effect with a 1.86-fold difference in ratio

seen between those with two "G" alleles at SNP rs13538 compared to those with two "A" alleles. This *NAT8* SNP has been associated by eQTL analysis with gene expression and is also a nonsynonymous SNP. We therefore investigate if this SNP has a direct functional role at the protein level by *in silico* modeling approaches.

Nonsynonymous NAT8 SNP Is Located in the Putative Substrate Binding Pocket of NAT8. Taking advantage of an AlphaFold[24] model of human NAT8 (Figure 6A), we probe the predicted 3D structure of this putative acetyltransferase and location of the nonsynonymous SNP (rs13538). The protein has a continuous pore (Figure 6 B,C) with two entrances. The channel is relatively large, with a predicted solvent accessible pore of 2604 Å^3. *In silico* docking of 4-Cl-KYN and acetyl-*co*-A (Figure 6 D,E) showed that the compounds utilize the breadth of the channel with the acetyl-*co*-A and 4-Cl-KYN in close proximity. The nonsynonymous SNP (rs13538) changes Phe to Ser at amino acid 143, which is located at the putative interface of where the acetyl-*co*-A and 4-Cl-KYN interact at the binding pocket (Figure 6 F). This could suggest an important functional role of amino acid 143 in substrate turnover that is altered in individuals with the Phe143Ser substitution.

◼ DISCUSSION

4-Cl-KYN is undergoing clinical development (NCT05280054) for a range of possible CNS-related indications. To aid in the development of this compound, we have identified and investigated a novel metabolite, ac-4-Cl-KYN. Once absorbed, 4-Cl-KYN is readily taken up across the BBB and converted to the active metabolite within astrocytes.[25−27] We found that ac-4-Cl-KYN had no effect on the transport activity of LAT1, indicating that this metabolite is unlikely to interfere with the uptake of 4-Cl-KYN across the BBB and, thus, will not affect the efficacy of the compound. This is similar to a finding by Nagamori et al. that found that *N*-acetyl-leucine does not interact with LAT1.[28] Our excretion studies found that 4-Cl-KYN and/or metabolites are excreted via urine. We found that ac-4-Cl-KYN inhibited multiple transporters expressed at the basolateral membrane of renal proximal tubules and the sinusoidal membrane of hepatocytes. OATs and OATP1B1 are important for the clearance of compounds from the plasma into the urine. *N*-Acetyl-leucine is also a substrate of OAT1 and OAT3.[28] A recent large-scale metabolome-wide association study (MWAS) approach has identified *SLC17A4* as a putative *N*-acetyl kynurenine transporter as an SNP located near this gene was associated with *N*-acetyl kynurenine levels in the blood.[29] SLC17A4 has been shown by both functional and genetic experiments to be a thyroid hormone transporter.[30,31]

The drug−drug interaction potential and direct transport studies should be investigated in further work. This would entail determining the percentage of unbound fraction of ac-4-Cl-KYN in plasma and the maximum plasma concentration (Cmax). This could then be combined with an experimentally determined IC50 value for transporter inhibition to determine the risk of a clinically relevant DDI as outlined by the FDA transporter-mediated drug−drug interaction guidelines. Also, a preclinical study to investigate if suppression of 4-Cl-KYN and its metabolites in the presence of ac-4-Cl-KYN occurs should be performed in the future.

We investigated the potential of a pharmacogenetic approach that could be used to stratify patients. In a recent

review article on psychiatry pharmacogenetics, Pardinas et al. argue for a focus on drug plasma concentrations, in particular on active drug metabolites, as this has the potential to correlate with drug efficacy and is a defined quantitative phenotype.[32] Due to sample size, we focused on key candidate genes that were selected from MWAS with the SNPs having a genetic association for nonchlorinated endogenous cellular metabolites of the compounds of interest in our current study.[29,33,34] Two associations were identified in our study: first, an *SLC7A5* SNP (rs28582913) was associated with 7-Cl-KYNA blood levels (*p* = 0.00667). rs28582913 is an intronic variant with eQTL analysis showing a link to *SLC7A5* gene expression in skin, tibial artery, and adipose tissue (GTEx Portal), with the CC allele having the lowest *SLC7A5* gene expression. This correlates with our study, where two CC alleles were associated with 46% lower blood concentrations. This suggests that LAT1 expression could be a rate-limiting factor for the generation of the active metabolite as its expression determines (restricts) how much of the parent drug is able to cross at the BBB and thus have access to cells that express kynurenine amino-transferase (KATs) (Figure 7). This is consistent with Lin et al., who found, in the nematode *Caenorhabditis elegans*, that neural production of kynurenic acid requires AAT-1, a homologue of LAT1.[35] In addition, a high-affinity transporter process for the uptake of KYN into astrocytes has been observed. This process was defined as being consistent with an LAT, but the specific transporter was not determined.[36,37] In summary, a replication study would need to be carried out to build on our genetic association identified in the present study for *SLC7A5* and to investigate if it correlates with the drug response.

Second, our data also revealed that the *NAT8* SNP, rs13538, was associated with the ratio of ac-4-Cl-KYN:4-Cl-KYN in plasma. NAT8 is predominantly expressed in the liver and kidneys and is involved in the removal of compounds by the addition of acetyl groups to amino acids or cystine conjugates to aid their excretion via bile or urine (Figure 7). rs13538, a nonsynonymous variant in NAT8, has been associated with circulating and urinary levels of n-acetyl-amino acids and has also been suggested as a susceptibility locus for chronic kidney disease.[38,39] It has been speculated that higher blood concentrations of *N*-acetyl amino acids can be indicative of chronic kidney disease.[39] As well as rs13538 being a nonsynonymous variant, eQTL analysis showed a link to *NAT8* gene expression in tissues such as nerve and adipose tissue (GTEx Portal) with the AA allele having the lowest *NAT8* gene expression with an additive effect for each additional G allele at this variant. This correlates with our findings as patients with a GG allele at this locus had a high ac-4-Cl-KYN:4-Cl-KYN ratio. As rs13538 is a nonsynonymous variant, we investigated the location of this amino acid change using the AlphaFold[24] predictive structural model of NAT8. *In silico* docking studies with the putative substrate, 4-Cl-KYN, and acetyl CoA found that they are in proximity within the binding pocket; in particular, the transfer point of acetyl from donor to substrate is located near the Phe143Ser variant. The only functional studies for NAT8 involve work that identified the enzymatic activity of NAT8 to add an acetyl group to cysteine s-conjugates.[40] Therefore, it would be interesting to perform functional experiments to confirm the direct metabolism of amino acid to n-acetyl compounds, as this has not been confirmed by enzyme-based metabolism assays and the involvement of the Phe143Ser variant. No other *NAT* gene
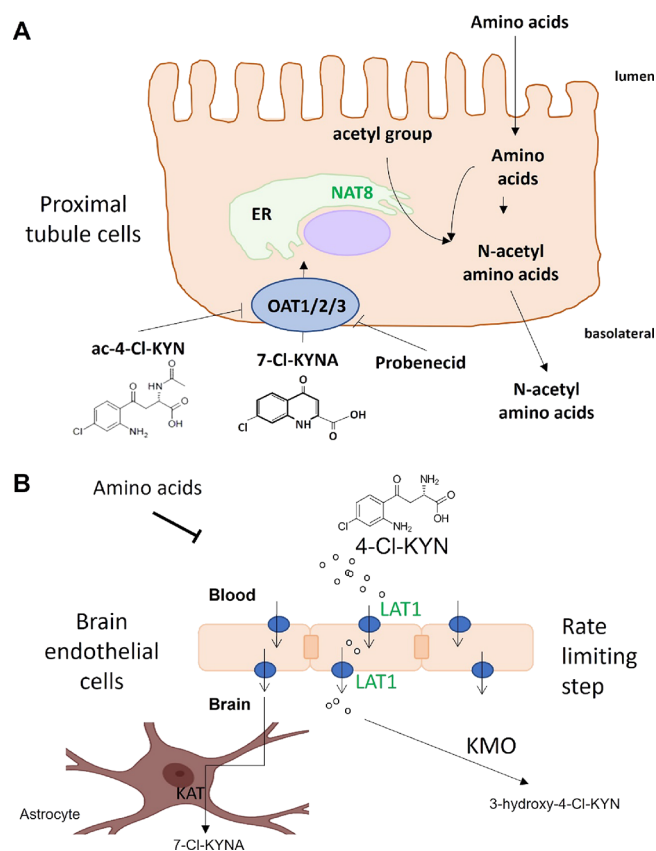
Figure 7. Passage of 4-Cl-KYN metabolites, 7-Cl-KYNA, and *N*-acetyl-4-Cl-KYN across renal proximal tubule cells and blood−brain barrier. (A) Diagram summarizing the passage of the metabolites of prodrug L-4-chlorokynurenine (4-Cl-KYN) across renal proximal tubule cells. The active metabolite, 7-chlorokynurenic acid (7-Cl-KYNA), is taken up into proximal tubule cells via organic anion transporters 1, 2, and 3 (OAT). Probenecid and the inactive metabolite of 4-Cl-KYN (*N*-acetyl-4-Cl-KYN) inhibit OATs to prevent the uptake of 7-Cl-KYNA across the basolateral membrane. Single-nucleotide polymorphism in *N*-acetyltransferase 8 (*NAT8*) is linked to the ratio of *N*-acetyl-4-Cl-KYN:4-Cl-KYN found in plasma. (B) Crossing of 4-Cl-KYN across the blood−brain barrier by LAT1 (SLC7A5) and metabolism to active metabolite (7-Cl-KYNA) in astrocytes or by KMO to 3-hydroxy-4-Cl-KYN. *SLC7A5* SNP is associated with the plasma level of 7-Cl-KYNA.

was investigated in the current study, as only *NAT8* has an association with the blood levels of acetylated-KYN.[29]

In our study, we have annotated our box and whisker plots of genetic associations with the self-identified ethnicity of the patients from the multicenter trial (ELEVATE) in the USA as our population cohort is 20% black. Underrepresented populations in pharmacogenetics are an active area of research as around 97% of GWAS data sets are of European ancestry while only 0.02% are of African American ethnicity.[41,42] For our study, ethnicity is known to alter the allele frequency for *NAT8*; i.e., the rs13538 major allele A has a frequency of 0.79 in Europeans but the allele frequency is 0.38 in Africans. As the field of MWAS expands, it will be interesting to investigate the relationship with ethnicity for the genes investigated, but larger patient cohorts would be required for this work.

Due to the species differences in activity for specific substrates such as with kynurenic acid,[23] we investigated the transport of 7-Cl-KYNA by rodent and human OATs. In addition to functional transport differences between species,

absolute proteomics studies for OAT expression in the kidney have shown protein expression differences.[43] For example, the level of expression of the OAT1 protein is higher in rat than in human kidney while that of the OAT2 protein is expressed in human kidney but not in rat. This could suggest that certain OATs are more important than others in the uptake of 7-Cl-KYNA, but further studies would be needed to determine this.

An ongoing clinical trial (NCT03078322) will determine, if in humans, the coadministration of probenecid with 4-Cl-KYN will boost the CNS concentrations of 7-Cl-KYNA. OATs are proposed to have a role in sensing and signaling, and so this would be an interesting avenue to investigate interorgan communication following the coadministration of probenecid.[44] How probenecid coadministration would affect the genetic associations found in the current study is unknown and would require a cohort of patients coadministered with both 4-Cl-KYN and probenecid to study this.

In this study, we used in vitro transporter assays, an animal study, and a human data set to investigate the transport and metabolism of 4-Cl-KYN, as this increased knowledge base will enhance the development of this therapeutic agent (Figure 7). For example, our finding of two genetic associations for drug concentration levels in plasma might enable a personalized medicine strategy for dosing, drug−drug interaction prediction, and/or patient stratification for drug response. Further replication cohorts and studies are required for this.

■ ASSOCIATED CONTENT

Ⓢ Supporting Information

The Supporting Information is available free of charge at https://pubs.acs.org/doi/10.1021/acs.molpharmaceut.3c00700.

Western blots for the expression of human and rat FLAG-OATs transiently transfected into HEK293 cells (PDF)

■ AUTHOR INFORMATION

Corresponding Author

David Dickens − *Department of Pharmacology and Therapeutics, University of Liverpool, Liverpool L69 3GL, United Kingdom;* ⓘ orcid.org/0000-0001-8295-0752; Phone: + 44 (0)151 795 5391; Email: david.dickens@liverpool.ac.uk

Authors

Waseema Patel − *Department of Pharmacology and Therapeutics, University of Liverpool, Liverpool L69 3GL, United Kingdom*

Ravi G. Shankar − *Institute of Population Health, University of Liverpool, Liverpool L69 3GL, United Kingdom*

Mark A. Smith − *Vistagen Therapeutics, Inc., South San Francisco, California 94080, United States; Medical College of Georgia, Augusta, Georgia 30912, United States*

H. Ralph Snodgrass − *Formerly at Vistagen Therapeutics, Inc., South San Francisco, California 94080, United States*

Munir Pirmohamed − *Department of Pharmacology and Therapeutics, University of Liverpool, Liverpool L69 3GL, United Kingdom*

Andrea L. Jorgensen − *Institute of Population Health, University of Liverpool, Liverpool L69 3GL, United Kingdom*

Ana Alfirevic − *Department of Pharmacology and Therapeutics, University of Liverpool, Liverpool L69 3GL, United Kingdom*

Complete contact information is available at:
https://pubs.acs.org/10.1021/acs.molpharmaceut.3c00700

■ ACKNOWLEDGMENTS

■ ABBREVIATIONS

4-Cl-KYN, 4-chlorokynurenine; 7-Cl-KYNA, 7-chlorokynurenic acid; BBB, blood−brain barrier; cGMP, cyclic guanosine monophosphate; DMEM, Dulbecco's modified Eagle's medium; E3S, estrone-3 sulfate; FBS, fetal bovine serum; HEK, human embryonic kidney; LAT1, L-type amino acid transporter; MADRS, Montgomery−Åsberg depression rating scale; ac-4-Cl-KYN, *N*-acetyl-4-chlorokynurenine; NAT8, *N*-acetyltransferase 8; OCT, organic cation transporter; OAT, organic anion transporter; PAGE, polyacrylamide gel electrophoresis; PAH, para-aminohippuric acid; PVDF, polyvinylidene fluoride; RIPA, radioimmunoprecipitation assay; SDS, sodium dodecyl sulfate; SNP, single-nucleotide polymorphism; TBS, Tris-buffered saline; TEA, tetraethylammonium

■ REFERENCES

(1) Gonda, X.; Dome, P.; Neill, J. C.; Tarazi, F. I. Novel antidepressant drugs: Beyond monoamine targets. *CNS Spectrums* **2021**, *28*, 1−10.

(2) Fava, M.; Davidson, K. G. Definition and epidemiology of treatment-resistant depression. *Psychiatr Clin North Am.* **1996**, *19* (2), 179−200.

(3) Kryst, J.; Kawalec, P.; Pilc, A. Efficacy and safety of intranasal esketamine for the treatment of major depressive disorder. *Expert Opin Pharmacother* **2020**, *21* (1), 9−20.

(4) Zanos, P.; Piantadosi, S. C.; Wu, H. Q.; Pribut, H. J.; Dell, M. J.; Can, A.; Snodgrass, H. R.; Zarate, C. A., Jr.; Schwarcz, R.; Gould, T. D. The Prodrug 4-Chlorokynurenine Causes Ketamine-Like Antidepressant Effects, but Not Side Effects, by NMDA/GlycineB-Site Inhibition. *J. Pharmacol Exp Ther* **2015**, *355* (1), 76−85.

(5) Bahr, R.; Lopez, A.; Rey, J. A. Intranasal Esketamine (Spravato™) for Use in Treatment-Resistant Depression In Conjunction With an Oral Antidepressant. *P T* **2019**, *44* (6), 340–375.

(6) Lapidus, K. A.; Levitch, C. F.; Perez, A. M.; Brallier, J. W.; Parides, M. K.; Soleimani, L.; Feder, A.; Iosifescu, D. V.; Charney, D. S.; Murrough, J. W. A randomized controlled trial of intranasal ketamine in major depressive disorder. *Biol. Psychiatry* **2014**, *76* (12), 970–6.

(7) Murphy, N.; Ramakrishnan, N.; Vo-Le, B.; Vo-Le, B.; Smith, M. A.; Iqbal, T.; Swann, A. C.; Mathew, S. J.; Lijffijt, M. A randomized cross-over trial to define neurophysiological correlates of AV-101 N-methyl-D-aspartate receptor blockade in healthy veterans. *Neuropsychopharmacology* **2021**, *46* (4), 820–827.

(8) Park, L. T.; Kadriu, B.; Gould, T. D.; Zanos, P.; Greenstein, D.; Evans, J. W.; Yuan, P.; Farmer, C. A.; Oppenheimer, M.; George, J. M.; Adeojo, L. W.; Snodgrass, H. R.; Smith, M. A.; Henter, I. D.; Machado-Vieira, R.; Mannes, A. J.; Zarate, C. A. A Randomized Trial of the N-Methyl-d-Aspartate Receptor Glycine Site Antagonist Prodrug 4-Chlorokynurenine in Treatment-Resistant Depression. *Int. J. Neuropsychopharmacol* **2020**, *23* (7), 417–425.

(9) Vistagen. *Vistagen Reports Topline Phase 2 Results for AV-101 as an Adjunctive Treatment of Major Depressive Disorder*. https://www.Vistagen.com/news-releases/news-release-details/Vistagen-reports-topline-phase-2-results-av-101-adjunctive 2019.

(10) Patel, W.; Rimmer, L.; Smith, M.; Moss, L.; Smith, M. A.; Snodgrass, H. R.; Pirmohamed, M.; Alfirevic, A.; Dickens, D. Probenecid Increases the Concentration of 7-Chlorokynurenic Acid Derived from the Prodrug 4-Chlorokynurenine within the Prefrontal Cortex. *Mol. Pharmaceutics* **2021**, *18* (1), 113–123.

(11) Bourque, M.; Gregoire, L.; Patel, W.; Dickens, D.; Snodgrass, R.; Di Paolo, T. AV-101, a Pro-Drug Antagonist at the NMDA Receptor Glycine Site, Reduces L-Dopa Induced dyskinesias in MPTP Monkeys. *Cells* **2022**, *11* (22), 3530 DOI: 10.3390/cells11223530.

(12) Wu, H. Q.; Lee, S. C.; Scharfman, H. E.; Schwarcz, R. L-4-chlorokynurenine attenuates kainate-induced seizures and lesions in the rat. *Experimental neurology* **2002**, *177* (1), 222–232.

(13) Yaksh, T. L.; Schwarcz, R.; Snodgrass, H. R. Characterization of the effects of L-4-chlorokynurenine on nociception in rodents. *J. Pain* **2017**, *14* (10), 1184–1196.

(14) Wallace, M.; White, A.; Grako, K. A.; Lane, R.; Cato, A. J.; Snodgrass, H. R. Randomized, double-blind, placebo-controlled, dose-escalation study: Investigation of the safety, pharmacokinetics, and antihyperalgesic activity of l-4-chlorokynurenine in healthy volunteers. *Scand J. Pain* **2017**, *17*, 243–251.

(15) Dickens, D.; Webb, S. D.; Antonyuk, S.; Giannoudis, A.; Owen, A.; Radisch, S.; Hasnain, S. S.; Pirmohamed, M. Transport of gabapentin by LAT1 (SLC7A5). *Biochem. Pharmacol.* **2013**, *85* (11), 1672–83.

(16) Dickens, D.; Chiduza, G. N.; Wright, G. S. A.; Pirmohamed, M.; Antonyuk, S. V.; Hasnain, S. S. Modulation of LAT1 (SLC7A5) transporter activity and stability by membrane cholesterol. *Sci. Rep.* **2017**, *7*, 43580.

(17) Liang, Z.; You, G. Chloroquine and Hydroxychloroquine, as Proteasome Inhibitors, Upregulate the Expression and Activity of Organic Anion Transporter 3. *Pharmaceutics* **2023**, *15* (6), 1725 DOI: 10.3390/pharmaceutics15061725.

(18) Xu, D.; Wang, H.; You, G. An Essential Role of Nedd4–2 in the Ubiquitination, Expression, and Function of Organic Anion Transporter-3. *Mol. Pharmaceutics* **2016**, *13* (2), 621–30.

(19) Tanaka, K.; Xu, W.; Zhou, F.; You, G. Role of glycosylation in the organic anion transporter OAT1. *J. Biol. Chem.* **2004**, *279* (15), 14961–6.

(20) Pardiñas, A. F.; Nalmpanti, M.; Pocklington, A. J.; Legge, S. E.; Medway, C.; King, A.; Jansen, J.; Helthuis, M.; Zammit, S.; MacCabe, J.; Owen, M. J.; O'Donovan, M. C.; Walters, J. T. R. Pharmacogenomic Variants and Drug Interactions Identified Through the Genetic Analysis of Clozapine Metabolism. *Am. J. Psychiatry* **2019**, *176* (6), 477–486.

(21) Valdes-Tresanco, M. S.; Valdes-Tresanco, M. E.; Valiente, P. A.; Moreno, E. AMDock: a versatile graphical tool for assisting molecular docking with AutoDock Vina and Autodock4. *Biol. Direct* **2020**, *15* (1), 12.

(22) Trott, O.; Olson, A. J. AutoDock Vina: improving the speed and accuracy of docking with a new scoring function, efficient optimization, and multithreading. *Journal of computational chemistry* **2010**, *31* (2), 455–61.

(23) Uwai, Y.; Hara, H.; Iwamoto, K. Transport of Kynurenic Acid by Rat Organic Anion Transporters rOAT1 and rOAT3: Species Difference between Human and Rat in OAT1. *Int. J. Tryptophan Res.* **2013**, *6*, 1–6.

(24) Jumper, J.; Evans, R.; Pritzel, A.; Green, T.; Figurnov, M.; Ronneberger, O.; Tunyasuvunakool, K.; Bates, R.; Zidek, A.; Potapenko, A.; Bridgland, A.; Meyer, C.; Kohl, S. A. A.; Ballard, A. J.; Cowie, A.; Romera-Paredes, B.; Nikolov, S.; Jain, R.; Adler, J.; Back, T.; Petersen, S.; Reiman, D.; Clancy, E.; Zielinski, M.; Steinegger, M.; Pacholska, M.; Berghammer, T.; Bodenstein, S.; Silver, D.; Vinyals, O.; Senior, A. W.; Kavukcuoglu, K.; Kohli, P.; Hassabis, D. Highly accurate protein structure prediction with AlphaFold. *Nature* **2021**, *596* (7873), 583–589.

(25) Wu, H. Q.; Salituro, F. G.; Schwarcz, R. Enzyme-catalyzed production of the neuroprotective NMDA receptor antagonist 7-chlorokynurenic acid in the rat brain in vivo. *European journal of pharmacology* **1997**, *319* (1), 13–20.

(26) Salituro, F. G.; Tomlinson, R. C.; Baron, B. M.; Palfreyman, M. G.; McDonald, I. A.; Schmidt, W.; Wu, H. Q.; Guidetti, P.; Schwarcz, R. Enzyme-activated antagonists of the strychnine-insensitive glycine/NMDA receptor. *J. Med. Chem.* **1994**, *37* (3), 334–6.

(27) Hokari, M.; Wu, H. Q.; Schwarcz, R.; Smith, Q. R. Facilitated brain uptake of 4-chlorokynurenine and conversion to 7-chlorokynurenic acid. *Neuroreport* **1996**, *8* (1), 15–8.

(28) Nagamori, S.; Wiriyasermkul, P.; Okuda, S.; Kojima, N.; Hari, Y.; Kiyonaka, S.; Mori, Y.; Tominaga, H.; Ohgaki, R.; Kanai, Y. Structure-activity relations of leucine derivatives reveal critical moieties for cellular uptake and activation of mTORC1-mediated signaling. *Amino acids* **2016**, *48* (4), 1045–1058.

(29) Yin, X.; Chan, L. S.; Bose, D.; Jackson, A. U.; VandeHaar, P.; Locke, A. E.; Fuchsberger, C.; Stringham, H. M.; Welch, R.; Yu, K.; Fernandes Silva, L.; Service, S. K.; Zhang, D.; Hector, E. C.; Young, E.; Ganel, L.; Das, I.; Abel, H.; Erdos, M. R.; Bonnycastle, L. L.; Kuusisto, J.; Stitziel, N. O.; Hall, I. M.; Wagner, G. R.; Ripatti, S.; Palotie, A.; Kang, J.; Morrison, J.; Burant, C. F.; Collins, F. S.; Ripatti, S.; Palotie, A.; Freimer, N. B.; Mohlke, K. L.; Scott, L. J.; Wen, X.; Fauman, E. B.; Laakso, M.; Boehnke, M. Genome-wide association studies of metabolites in Finnish men identify disease-relevant loci. *Nat. Commun.* **2022**, *13* (1), 1644.

(30) Groeneweg, S.; van Geest, F. S.; Chen, Z.; Farina, S.; van Heerebeek, R. E. A.; Meima, M. E.; Peeters, R. P.; Heuer, H.; Medici, M.; Visser, W. E. Functional Characterization of the Novel and Specific Thyroid Hormone Transporter SLC17A4. *Thyroid* **2022**, *32* (3), 326–335.

(31) Teumer, A.; Chaker, L.; Groeneweg, S.; Li, Y.; Di Munno, C.; Barbieri, C.; Schultheiss, U. T.; Traglia, M.; Ahluwalia, T. S.; Akiyama, M.; Appel, E. V. R.; Arking, D. E.; Arnold, A.; Astrup, A.; Beekman, M.; Beilby, J. P.; Bekaert, S.; Boerwinkle, E.; Brown, S. J.; De Buyzere, M.; Campbell, P. J.; Ceresini, G.; Cerqueira, C.; Cucca, F.; Deary, I. J.; Deelen, J.; Eckardt, K. U.; Ekici, A. B.; Eriksson, J. G.; Ferrrucci, L.; Fiers, T.; Fiorillo, E.; Ford, I.; Fox, C. S.; Fuchsberger, C.; Galesloot, T. E.; Gieger, C.; Gögele, M.; De Grandi, A.; Grarup, N.; Greiser, K. H.; Haljas, K.; Hansen, T.; Harris, S. E.; van Heemst, D.; den Heijer, M.; Hicks, A. A.; den Hollander, W.; Homuth, G.; Hui, J.; Ikram, M. A.; Ittermann, T.; Jensen, R. A.; Jing, J.; Jukema, J. W.; Kajantie, E.; Kamatani, Y.; Kasbohm, E.; Kaufman, J. M.; Kiemeney, L. A.; Kloppenburg, M.; Kronenberg, F.; Kubo, M.; Lahti, J.; Lapauw, B.; Li, S.; Liewald, D. C. M.; Alizadeh, B. Z.; Boezen, H. M.; Franke, L.; van der Harst, P.; Navis, G.; Rots, M.; Snieder, H.; Swertz, M. A.;

Wijmenga, C.; Lim, E. M.; Linneberg, A.; Marina, M.; Mascalzoni, D.; Matsuda, K.; Medenwald, D.; Meisinger, C.; Meulenbelt, I.; De Meyer, T.; Meyer zu Schwabedissen, H. E.; Mikolajczyk, R.; Moed, M.; Netea-Maier, R. T.; Nolte, I. M.; Okada, Y.; Pala, M.; Pattaro, C.; Pedersen, O.; Petersmann, A.; Porcu, E.; Postmus, I.; Pramstaller, P. P.; Psaty, B. M.; Ramos, Y. F. M.; Rawal, R.; Redmond, P.; Richards, J. B.; Rietzschel, E. R.; Rivadeneira, F.; Roef, G.; Rotter, J. I.; Sala, C. F.; Schlessinger, D.; Selvin, E.; Slagboom, P. E.; Soranzo, N.; Sørensen, T. I. A.; Spector, T. D.; Starr, J. M.; Stott, D. J.; Taes, Y.; Taliun, D.; Tanaka, T.; Thuesen, B.; Tiller, D.; Toniolo, D.; Uitterlinden, A. G.; Visser, W. E.; Walsh, J. P.; Wilson, S. G.; Wolffenbuttel, B. H. R.; Yang, Q.; Zheng, H. F.; Cappola, A.; Peeters, R. P.; Naitza, S.; Völzke, H.; Sanna, S.; Köttgen, A.; Visser, T. J.; Medici, M. Genome-wide analyses identify a role for SLC17A4 and AADAT in thyroid hormone regulation. *Nat. Commun.* **2018**, *9* (1), 4455.

(32) Pardinas, A. F.; Owen, M. J.; Walters, J. T. R. Pharmacogenomics: A road ahead for precision medicine in psychiatry. *Neuron* **2021**, *109* (24), 3914–3929.

(33) Shin, S. Y.; Fauman, E. B.; Petersen, A. K.; Krumsiek, J.; Santos, R.; Huang, J.; Arnold, M.; Erte, I.; Forgetta, V.; Yang, T. P.; Walter, K.; Menni, C.; Chen, L.; Vasquez, L.; Valdes, A. M.; Hyde, C. L.; Wang, V.; Ziemek, D.; Roberts, P.; Xi, L.; Grundberg, E.; Waldenberger, M.; Richards, J. B.; Mohney, R. P.; Milburn, M. V.; John, S. L.; Trimmer, J.; Theis, F. J.; Overington, J. P.; Suhre, K.; Brosnan, M. J.; Gieger, C.; Kastenmüller, G.; Spector, T. D.; Soranzo, N. An atlas of genetic influences on human blood metabolites. *Nat. Genet.* **2014**, *46* (6), 543–550.

(34) Long, T.; Hicks, M.; Yu, H. C.; Biggs, W. H.; Kirkness, E. F.; Menni, C.; Zierer, J.; Small, K. S.; Mangino, M.; Messier, H.; Brewerton, S.; Turpaz, Y.; Perkins, B. A.; Evans, A. M.; Miller, L. A.; Guo, L.; Caskey, C. T.; Schork, N. J.; Garner, C.; Spector, T. D.; Venter, J. C.; Telenti, A. Whole-genome sequencing identifies common-to-rare variants associated with human blood metabolites. *Nature genetics* **2017**, *49* (4), 568–578.

(35) Lin, L.; Lemieux, G. A.; Enogieru, O. J.; Giacomini, K. M.; Ashrafi, K. Neural production of kynurenic acid in Caenorhabditis elegans requires the AAT-1 transporter. *Genes & development* **2020**, *34* (15–16), 1033–1038.

(36) Kiss, C.; Ceresoli-Borroni, G.; Guidetti, P.; Zielke, C. L.; Zielke, H. R.; Schwarcz, R. Kynurenate production by cultured human astrocytes. *J. Neural Transm (Vienna)* **2003**, *110* (1), 1–14.

(37) Speciale, C.; Hares, K.; Schwarcz, R.; Brookes, N. High-affinity uptake of L-kynurenine by a Na+-independent transporter of neutral amino acids in astrocytes. *J. Neurosci.* **1989**, *9* (6), 2066–72.

(38) Chambers, J. C.; Zhang, W.; Lord, G. M.; van der Harst, P.; Lawlor, D. A.; Sehmi, J. S.; Gale, D. P.; Wass, M. N.; Ahmadi, K. R.; Bakker, S. J.; Beckmann, J.; Bilo, H. J.; Bochud, M.; Brown, M. J.; Caulfield, M. J.; Connell, J. M.; Cook, H. T.; Cotlarciuc, I.; Davey Smith, G.; de Silva, R.; Deng, G.; Devuyst, O.; Dikkeschei, L. D.; Dimkovic, N.; Dockrell, M.; Dominiczak, A.; Ebrahim, S.; Eggermann, T.; Farrall, M.; Ferrucci, L.; Floege, J.; Forouhi, N. G.; Gansevoort, R. T.; Han, X.; Hedblad, B.; Homan van der Heide, J. J.; Hepkema, B. G.; Hernandez-Fuentes, M.; Hypponen, E.; Johnson, T.; de Jong, P. E.; Kleefstra, N.; Lagou, V.; Lapsley, M.; Li, Y.; Loos, R. J.; Luan, J.; Luttropp, K.; Marechal, C.; Melander, O.; Munroe, P. B.; Nordfors, L.; Parsa, A.; Peltonen, L.; Penninx, B. W.; Perucha, E.; Pouta, A.; Prokopenko, I.; Roderick, P. J.; Ruokonen, A.; Samani, N. J.; Sanna, S.; Schalling, M.; Schlessinger, D.; Schlieper, G.; Seelen, M. A.; Shuldiner, A. R.; Sjogren, M.; Smit, J. H.; Snieder, H.; Soranzo, N.; Spector, T. D.; Stenvinkel, P.; Sternberg, M. J.; Swaminathan, R.; Tanaka, T.; Ubink-Veltmaat, L. J.; Uda, M.; Vollenweider, P.; Wallace, C.; Waterworth, D.; Zerres, K.; Waeber, G.; Wareham, N. J.; Maxwell, P. H.; McCarthy, M. I.; Jarvelin, M. R.; Mooser, V.; Abecasis, G. R.; Lightstone, L.; Scott, J.; Navis, G.; Elliott, P.; Kooner, J. S. Genetic loci influencing kidney function and chronic kidney disease. *Nat. Genet.* **2010**, *42* (5), 373–375.

(39) Luo, S.; Surapaneni, A.; Zheng, Z.; Rhee, E. P.; Coresh, J.; Hung, A. M.; Nadkarni, G. N.; Yu, B.; Boerwinkle, E.; Tin, A.; Arking, D. E.; Steinbrenner, I.; Schlosser, P.; Kottgen, A.; Grams, M. E. NAT8 Variants, N-Acetylated Amino Acids, and Progression of CKD. *Clinical journal of the American Society of Nephrology: CJASN* **2021**, *16* (1), 37–47.

(40) Veiga-da-Cunha, M.; Tyteca, D.; Stroobant, V.; Courtoy, P. J.; Opperdoes, F. R.; Van Schaftingen, E. Molecular identification of NAT8 as the enzyme that acetylates cysteine S-conjugates to mercapturic acids. *J. Biol. Chem.* **2010**, *285* (24), 18888–98.

(41) Sirugo, G.; Williams, S. M.; Tishkoff, S. A. The Missing Diversity in Human Genetic Studies. *Cell* **2019**, *177* (1), 26–31.

(42) Pirmohamed, M. Pharmacogenomics: current status and future perspectives. *Nature reviews. Genetics* **2023**, *24*, 350–362.

(43) Basit, A.; Radi, Z.; Vaidya, V. S.; Karasu, M.; Prasad, B. Kidney Cortical Transporter Expression across Species Using Quantitative Proteomics. *Drug metabolism and disposition: the biological fate of chemicals* **2019**, *47* (8), 802–808.

(44) Nigam, S. K.; Granados, J. C. OAT, OATP, and MRP Drug Transporters and the Remote Sensing and Signaling Theory. *Annual review of pharmacology and toxicology* **2023**, *63*, 637–660.